ELSEVIER

Journal of Photochemistry and Photobiology A: Chemistry 94 (1996) 93–100

Journal of
PHOTOCHEMISTRY
AND
PHOTOBIOLOGY
A: CHEMISTRY

# Dependence of the intramolecular electronic energy transfer in bichromophoric molecules on the interchromophore bridge

Eva Toledano, Mordecai B. Rubin *, Shammai Speiser *

*Department of Chemistry, Technion - Israel Institute of Technology, Haifa 32000, Israel*

Received 31 January 1995; accepted 22 June 1995

## Abstract

Results are presented on the intramolecular electronic energy transfer (intra-EET) in bichromophoric molecules of the type benzene–$\alpha$-diketone, in which the interchromophore bridge contains methyl substituents $\beta$ to the $\alpha$-dicarbonyl acceptor chromophore. These results show that singlet–singlet intra-EET is independent of substitution and can be explained by a model assuming Dexter-type short-range exchange interaction. For singlet–triplet and triplet–triplet transfer, there are indications that the phosphorescence yield of the acceptor is larger than that for non-substituted bichromophoric molecules. This can be explained by through-bond interaction promoting EET via a long-range superexchange mechanism, by variations in the non-radiative decay of the triplet state of the acceptor or by chemical reaction.

*Keywords:* Intramolecular electronic energy transfer; Bichromophoric molecules; Inter-chromophore bridge

## 1. Introduction

The photophysics of bichromophoric molecules of the type donor–bridge–acceptor (D–B–A) involves interaction between the excited donor chromophore (D*) and the ground state acceptor chromophore. This interaction may lead to the observation of phenomena such as intramolecular excimer formation, intramolecular electronic energy transfer (intra-EET) and intramolecular electron transfer (intra-ELT) [1–5]. The role of the bridge in promoting these transfer processes has been discussed and the possibility of long-range superexchange involving through-bond (TB) interaction has been suggested as a suitable mechanism to describe some of the characteristics observed [6–11]. Recently, we have studied the D–B–A molecular systems P-4,4 and P-5,5, shown in Fig. 1, and have compared them with similar benzene–$\alpha$-diketone bichromophoric molecules in which the macrocylic methylene unit bridge was varied; this enables intra-EET to be investigated as a function of the interchromophore distance $R$ and the relative orientation of the two chromophores [12–15]. All of the observations can be rationalized in terms of a short-range transfer mechanism involving Dexter-type exchange interaction [16], without considering the TB interaction involving the interchromophore bridge.

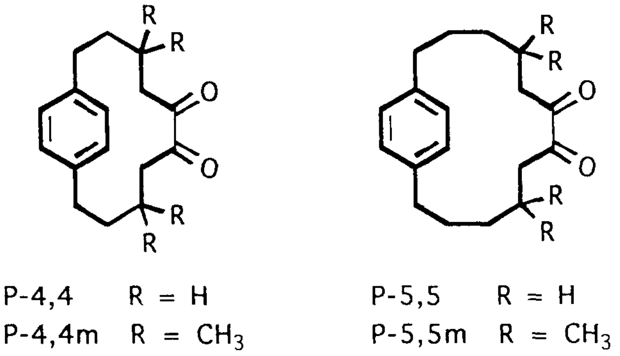

Fig. 1. The bichromophoric molecules investigated in this study.

In this paper, we report the results of intra-EET studies in the tetramethyl-substituted bichromophoric molecules P-4,4m and P-5,5m, shown in Fig. 1, which can be compared with those obtained for P-4,4 and P-5,5. The methyl substitution $\beta$ to the carbonyl groups perturbs the electronic structure of the bridge system, so that any TB interaction may be manifested as a difference between the intra-EET efficiencies for P-4,4m and P-5,5m compared with P-4,4 and P-5,5.

## 2. Experimental details

The experimental apparatus was similar to that used in previous studies of intra-EET [12,13,17]. The P-4,4m and

---

* Corresponding authors.

*SSDI* 1010-6030(95)04147-8

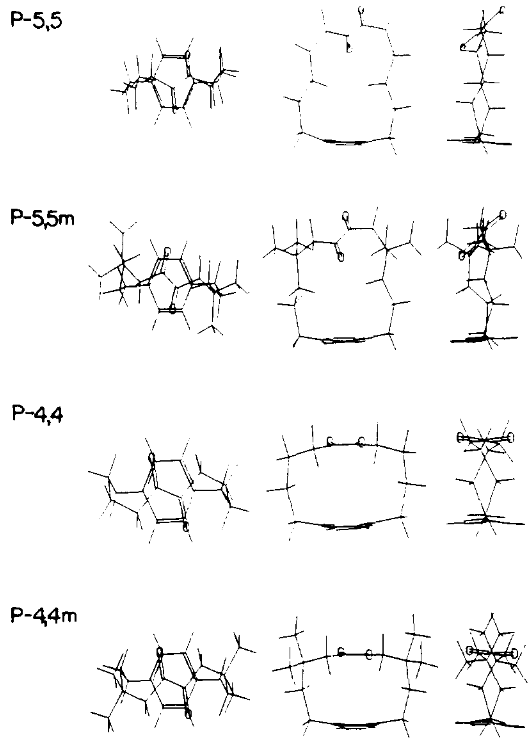

Fig. 2. Molecular stereographic projections obtained from Batch-Min V.3.1-MM2 force-field calculations.

P-5,5m samples were obtained from the laboratory of Professor R. Gleiter, University of Heidelberg.

## 3. Results

### 3.1. Molecular structures

The molecular structures of P-4,4, P-4,4m, P-5,5 and P-5,5m were determined by X-ray crystallography (except for P-5,5) (details of the structural determinations are available from Dr. M. Kapon, Department of Chemistry, Technion - Israel Institute of Technology, Haifa 32000, Israel) and by MM2 force-field calculations. The structures obtained in the calculations are shown in Fig. 2 and the geometrical parameters for the molecules are summarized in Table 1. Since the geometries of P-4,4 and P-4,4m are very similar, any difference in intra-EET efficiency can be attributed to differences involving the electronic structure of the bridge. The geometrical differences between P-5,5 and P-5,5m are too large to allow such conclusions.

### 3.2. Absorption spectra

All the bichromophoric molecules shown in Fig. 1 have similar absorption spectra with two bands: one at 420–460 nm, typical of α-diketone $n_+ \rightarrow \pi^*$ absorption, and one at 260–280 nm, typical of the benzene chromophore. These spectra are similar to those observed for all other benzene–α-diketone bichromophoric molecules studied in our laboratory, and are basically a superposition of the absorption spectra of the separate chromophores [12,13,17]. There is no indication of any interaction between the chromophores in the ground electronic states nor of any coupling between interchromophoric bridge electronic states.

Table 1
The geometrical parameters [15] defining the orientation of the chromophores and the dihedral angle between the carbonyls, calculated from the structures obtained by Batch-Min V.3.1.-MM2 force-field calculations, and the energy of the conformation

| Parameter | | Molecule | | | |
|---|---|---|---|---|---|
| | | P-4,4m | P-4,4 | P-5,5m | P-5,5 |
| $R$ (Å) | | 3.20 | 3.28 | 4.94 | 5.36 |
| $\theta$ (°) | Translation matrix [a] | 0.005 | 0.84 | 0.48 | 5.44 |
| $\phi$ (°) | | −46.93 | −18.45 | 7.18 | 75.39 |
| $\theta$ (°) | | 0.38 | 0.85 | 34.90 | 33.00 |
| $\phi$ (°) | Rotation matrix [a] | 50.04 | 18.43 | −14.31 | 8.44 |
| $\chi$ (°) | | 171.86 | 140.39 | 82.88 | 96.44 |
| Dihedral angle (°) | | 174 | 170 | 177 | 175 |
| Energy (kJ mol$^{-1}$) | | 110.5 | 83.8 | 112.1 | 78.5 |

[a] For definition, see Ref. [15].

### 3.3. Emission spectra

The time-resolved emission spectra are shown in Fig. 3. The quantum yields of fluorescence ($\Phi_F$) and phosphorescence ($\Phi_P$) of the bichromophoric molecules after excitation of either the benzene chromophore ($\lambda_{ex}$ = 268 nm) or the α-diketone chromophore ($\lambda_{ex}$ = 430 nm) are shown in Table 2. The results are given for the emission of both chromophores, and are compared with those for the separate acceptor chromophore ($\Phi^0$(A)). These results were obtained by integration of the corresponding corrected emission bands. With the exception of P-5,5, no donor (benzene) fluorescence is observed and only the α-diketone fluorescence at 460–495 nm is detected, indicating very efficient singlet–singlet intra-EET. The fluorescence yield for this emission is higher for 430 nm excitation than for 268 nm excitation which involves intra-EET. P-5,5 shows a dual fluorescence spectrum similar to that observed for other bichromophoric molecules.

The phosphorescence spectra show only α-diketone emission at 530–650 nm. The quantum yields for P-4,4 and P-5,5 are higher than those for P-4,4m and P-5,5m when excitation is at the benzene site, involving triplet–triplet intra-EET, and lower than those for P-4,4m and P-5,5m when excitation is at the α-diketone absorption band.

### 3.4. Excitation spectra

The excitation spectra of the bichromophoric molecules, recorded by monitoring the α-diketone emission and normalized to the absorption of the benzene chromophore, are shown in Fig. 4. These spectra are similar to the absorption spectra, which are the same for all the molecules. Thus the

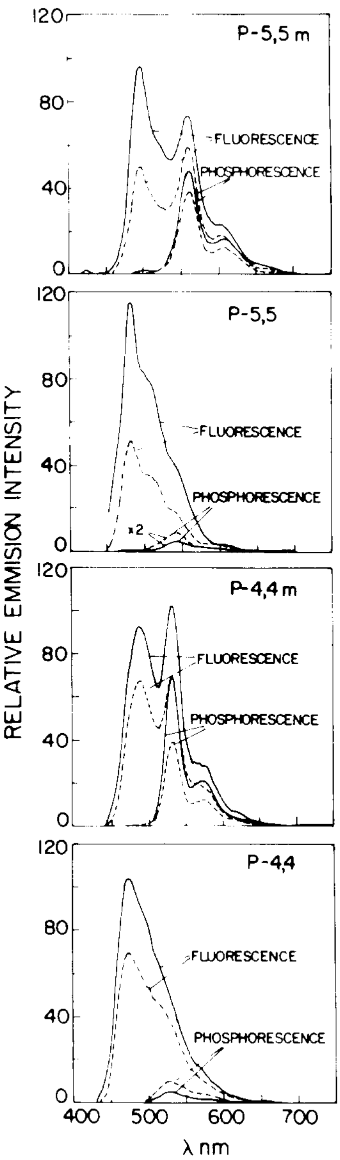

Fig. 3. Time-resolved emission spectroscopy of the $\alpha$-diketone chromophore excited at 268 nm at the benzene donor site (full line) and at 430 nm at the acceptor $\alpha$-diketone chromophore site (broken line) at 298 K.

observed variations are indicative of the intra-EET process which is dependent on the molecular structure.

### 3.5. Phosphorescence lifetimes of the α-diketone chromophore

The phosphorescence lifetimes of the $\alpha$-diketone chromophore were measured at 298 and 80 K exciting either one of the two chromophores. The results are summarized in Table 3. The measured lifetimes for biacetyl are similar to those reported in the literature.

### 3.6. Efficiency of the singlet–singlet intra-EET process

The efficiency of the singlet–singlet intra-EET process in the bichromophoric molecules can be determined from measurements of the quenching of the benzene (donor) fluorescence or the enhancement of the $\alpha$-diketone (acceptor) fluorescence on donor excitation. The transfer efficiency is expressed in terms of $Q_{ET}^{SS}$ [12,13,17]

$$Q_{ET}^{SS} = 1 - \frac{\Phi_F^{ET}(D)}{\Phi_F^{0}(D)} = \frac{\Phi_F^{ET}(A)}{\Phi_F^{0}(A)} \qquad (1)$$

where $\Phi_F^{ET}(D)$ denotes the fluorescence quantum yield of the donor in the bichromophoric molecules and $\Phi_F^{0}(D)$ is the corresponding value for the separate donor ($p$-xylene) chromophore. $Q_{ET}^{SS}$ is determined from the ratio between the fluorescence quantum yield of the acceptor following donor excitation and the intra-EET process ($\Phi_F^{ET}(A)$) to that obtained by direct excitation of the acceptor chromophore at the same wavelength ($\Phi_F^{0}(A)$). The results are given in Table 4, together with an estimate of the singlet–singlet intra-EET rate constant $k_{ET}^{SS}$ given by

$$k_{ET}^{SS} = \frac{Q_{ET}^{SS}}{1 - Q_{ET}^{SS}} \frac{1}{\tau_D} \qquad (2)$$

where $\tau_D$ is the fluorescence lifetime of the donor chromophore. Similar values for the transfer efficiency were obtained from the measured excitation spectra (Fig. 4).

### 3.7. Efficiency of the triplet–triplet and singlet–triplet intra-EET processes

Estimates of the efficiency of the intra-EET process to acceptor triplet states in the bichromophoric molecules were determined from the ratio $\rho^{ET}$ between the phosphorescence and fluorescence quantum yields of the $\alpha$-diketone chromophore, obtained as a result of intra-EET, to the ratio $\rho^{D}$ obtained as a result of direct excitation of the $\alpha$-diketone. The results are expressed in terms of the triplet transfer parameter $\xi^{T\text{-}T}$ defined by [13]

$$\xi^{T-T} = \frac{\rho^{ET}}{\rho^{D}} = 1 + \frac{Q_{ET}^{SS} + Q_{ET}^{TT}}{(Q_{ET}^{SS} + Q_{ET}^{TS})\,\tau_A k_{ISC}^{A}} \qquad (3)$$

where $Q$ is the transfer efficiency in each of the energy transfer routes, singlet–singlet (SS), triplet–triplet (TT), singlet–triplet (ST) and triplet–singlet (TS), $k_{ISC}^{A}$ is the intersystem crossing rate for the acceptor chromophore and $\tau_A$ is the fluorescence lifetime of the acceptor. The results are summarized in Table 5. Triplet–triplet and singlet–triplet transfer processes are manifested by $\xi^{T\text{-}T} > 1$ within experimental error; these are observed only for the bichromophoric molecules in which the interchromophore bridge is not substituted by $\beta$-methyl groups.

### 3.8. Temperature dependence of the emission spectra and transfer efficiencies

The dependence of the donor fluorescence yield was measured in the temperature range 160–298 K. Since the fluorescence quantum yield of xylene is independent of temperature,

Table 2
Experimental results of the emission spectra and relative emission yields of the bichromophoric molecules and their constituent chromophores

| Molecule | Fluorescence | | | Phosphorescence | |
|---|---|---|---|---|---|
| | $\lambda_{ex}=268$ nm $\Phi_F(D)$ | $\lambda_{ex}=268$ nm $\Phi_F^{ET}(A)$ | $\lambda_{ex}=430$ nm $\Phi_F^0(A)$ | $\lambda_{ex}=268$ nm $\Phi_P^{ET}(A)$ | $\lambda_{ex}=430$ nm $\Phi_P^0(A)$ |
| P-4,4 | – | 197900 | 298200 | 21350 | 11200 |
| P-4,4m | – | 171000 | 238000 | 53960 | 95890 |
| P-5,5 | 1196000 | 119000 | 243900 | 5700 | 3960 |
| P-5,5m | – | 105200 | 187700 | 46300 | 62200 |
| *p*-Xylene | 10973000 | – | – | – | – |
| Biacetyl | – | – | 239900 | – | 115000 |

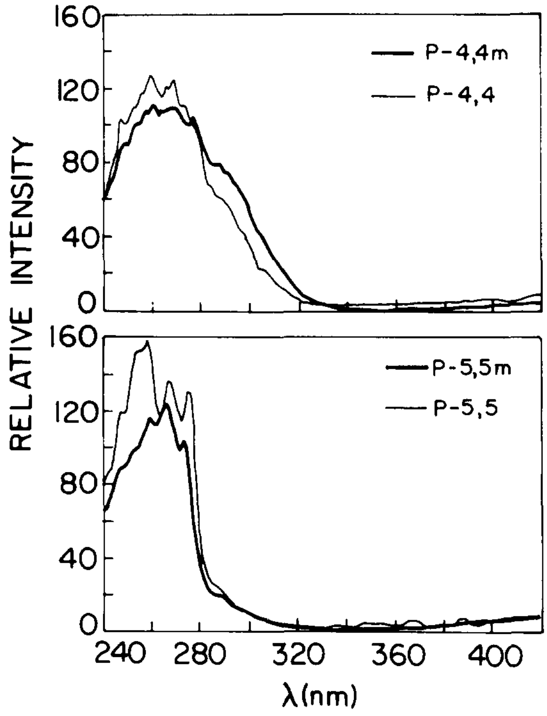

Fig. 4. Fluorescence excitation spectra of P-4,4, P-4,4m, P-5,5 and P-5,5m.

Table 3
Measured phosphorescence lifetimes for the α-diketone chromophore at 298 and 80 K

| Molecule | $\lambda_{ex}$ (nm) | Temperature (K) | $\tau_D$ (ms) |
|---|---|---|---|
| P-4,4 | 268 | 298 | 0.018 ± 0.003 |
| | 430 | 298 | 0.016 ± 0.003 |
| | 430 | 80 | 4.000 ± 0.5 |
| P-4,4m | 268 | 298 | 0.178 ± 0.002 |
| | 430 | 298 | 0.222 ± 0.002 |
| | 430 | 80 | 4.500 ± 0.5 |
| P-5,5 | 268 | 298 | 0.011 ± 0.003 |
| | 430 | 298 | 0.011 ± 0.003 |
| | 430 | 80 | 2.500 ± 0.5 |
| P-5,5m | 268 | 298 | 0.097 ± 0.002 |
| | 430 | 298 | 0.111 ± 0.002 |
| | 430 | 80 | 1.800 ± 0.5 |
| Biacetyl | 422 | 298 | 0.200 ± 0.02 |
| | 422 | 80 | 1.100 ± 0.3 |

variations in the quantum yield can be attributed to the temperature- dependent intra-EET process. For P-5,5, the fluorescence quantum yield shows a monotonic decrease with temperature (Fig. 5), whereas for P-5,5m, P-4,4 and P-4,4m, no temperature dependence is observed.

Table 4
The energy transfer efficiency $Q_{ET}^{SS}$ and the rate of energy transfer $k_{ET}^{SS}$ (Eqs. (1) and (2)) calculated from the emission spectra at 298 K

| Molecule | $Q_{ET}^{SS}(D)$ | $k_{ET}^{SS}(D)$ ($10^9$ s$^{-1}$) | $Q_{ET}^{SS}(D)$ | $k_{ET}^{SS}(A)$ ($10^7$ s$^{-1}$) |
|---|---|---|---|---|
| P-4,4 | 1 | $\geqslant 3$ | 0.66 ± 0.1 | 6 ± 2 |
| P-4,4m | 1 | $\geqslant 3$ | 0.71 ± 0.1 | 8 ± 2 |
| P-5,5 | 0.89 ± 0.02 | 0.3 ± 0.05 | 0.49 ± 0.1 | 3 ± 2 |
| P-5,5m | 1 | $\geqslant 3$ | 0.56 ± 0.1 | 4 ± 2 |

Table 5
Ratio $\rho^{ET}$ between the quantum yield of phosphorescence and fluorescence of the α-diketone chromophore obtained by excitation of the donor chromophore, the same ratio obtained by direct excitation of the α-diketone chromophore ($\rho^D$) and the $\xi^{T\text{-}T}$ parameter

| Molecule | $\rho^{ET}$ | $\rho^D$ | $\xi^{T\text{-}T}$ |
|---|---|---|---|
| P-4,4 | 0.11 | 0.037 | 2.1 ± 0.5 |
| P-4,4m | 0.32 | 0.40 | 0.8 ± 0.3 |
| P-5,5 | 0.048 | 0.016 | 2.9 ± 0.5 |
| P-5,5m | 0.44 | 0.33 | 1.4 ± 0.4 |

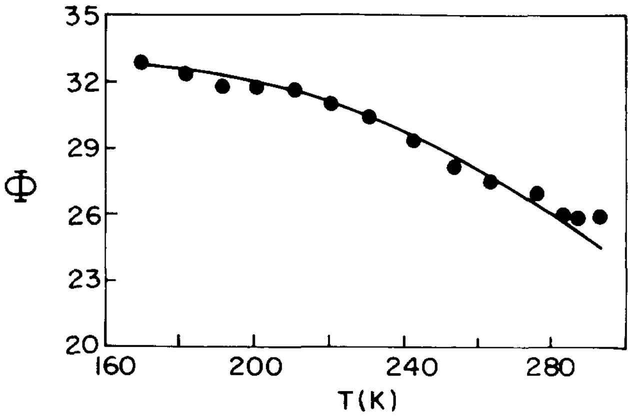

Fig. 5. Temperature-dependent relative fluorescence quantum yield of the aromatic chromophore of the molecule P-5,5.

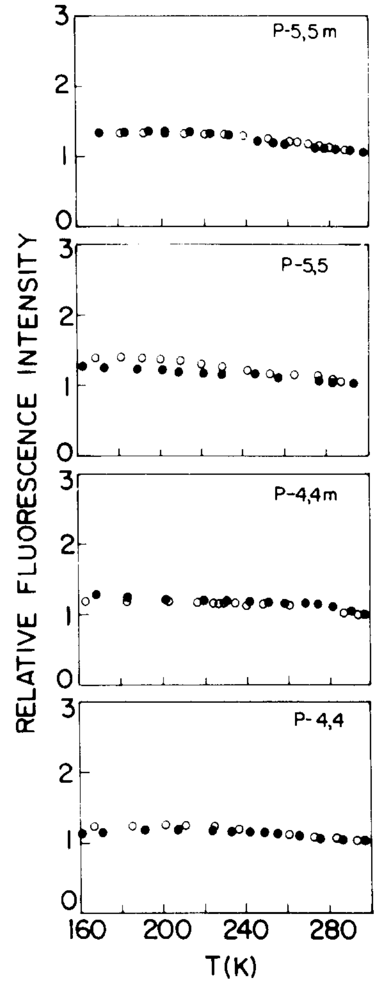

Fig. 6. Temperature-dependent fluorescence intensity for the $\alpha$-diketone chromophore at the excitation wavelengths of 268 nm (●) and 430 nm (○). The intensities are normalized to that at 298 K.

These results are in agreement with previous investigations on this bichromophoric molecular series [12,17]. The variations of $\Phi_F$ with temperature are a result of temperature-activated conformational change. The activation energy for such a change in P-5,5, obtained from the fitting of Fig. 5 to such a model, is $\Delta E = 1050 \pm 80$ cm$^{-1}$. The temperature dependence of the $\alpha$-diketone fluorescence, excited at either 268 or 430 nm, is shown in Fig. 6. It is typical of other $\alpha$-diketones, such as biacetyl, and does not reflect any temperature-dependent intra-EET. The slight increase in $\Phi$ on 268 nm excitation of P-5,5 is consistent with the temperature dependence of $\Phi$ for the donor fluorescence (Fig. 5).

The temperature dependence of the phosphorescence yield, shown in Fig. 7, is in good agreement with the lifetime data (Table 3). The $\beta$-methyl substitution in the bridge has a marked influence on the phosphorescence yield at both excitation wavelengths. The triplet transfer parameters are obtained (Fig. 8) from the measured temperature- dependent fluorescence and phosphorescence. We see that $\xi^{T\text{-}T}$ is temperature independent for the methyl-substituted bichromophoric molecules, but increases with temperature for P-4,4 and P-5,5.

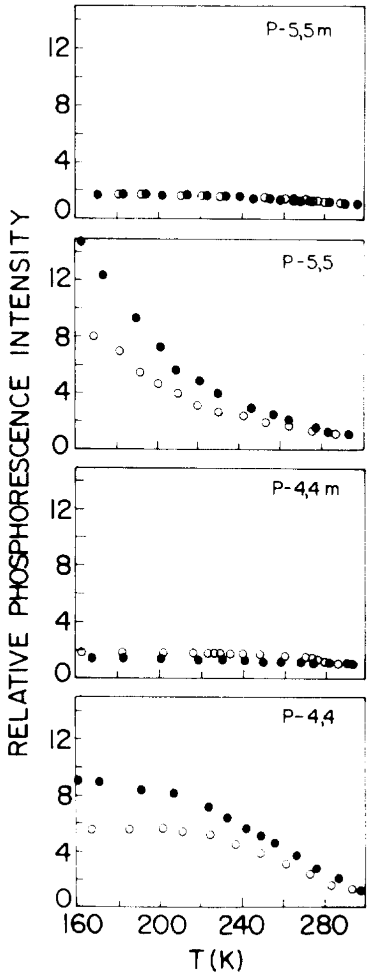

Fig. 7. Temperature-dependent phosphorescence intensity for the $\alpha$-diketone chromophore at the excitation wavelengths of 268 nm (●) and 430 nm (○). The intensities are normalized to that at 298 K.

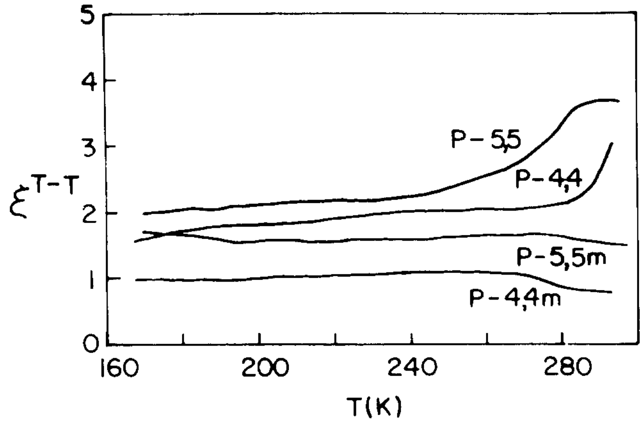

Fig. 8. Temperature dependence of $\xi^{T\text{-}T}$.

## 4. Discussion

Fig. 9 shows the energy level diagram and kinetic scheme for the photophysical processes involving the $p$-xylene–bi acetyl system. Using this scheme and the absorption and emission spectra, we can determine the relevant singlet–sin-

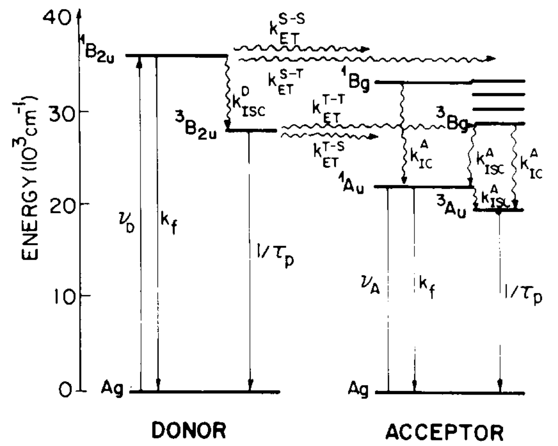

Fig. 9. Schematic energy level diagram for describing singlet–singlet, singlet–triplet, triplet–triplet and triplet–singlet intra-ET in a donor–acceptor bichromophoric molecule. The donor (*p*-xylene) and the acceptor (biacetyl) can be excited separately by choosing the corresponding excitation frequency, $\nu_D$ and $\nu_A$ respectively. $k_{ET}$ denotes intra-ET rates, $k_{ISC}$ denotes ISC rates, $k_{IC}$ denotes IC rates, $k_F$ is the sum of $S_1 \rightarrow S_0$ decay rates and $\tau_P$ is the corresponding phosphorescence lifetime.

glet and triplet–triplet decay routes in the bichromophoric molecules. From the spectra, the spectral overlap integral for dipole–dipole Förster- type [4] long-range EET ($J_{d\text{-}d}$) and for short-range Dexter-type EET through exchange interaction ($J_{ex}$) can be determined. These integrals are defined by [5]

$$J_{d-d}=\frac{\int F_D(\bar{\nu})\epsilon_A(\bar{\nu})\bar{\nu}^{-4}\,d\bar{\nu}}{\int F_D(\bar{\nu})\,d\bar{\nu}} \tag{4}$$

$$J_{ex}=\frac{\int F_D(\bar{\nu})\epsilon_A(\bar{\nu})\,d\bar{\nu}}{\int F_D(\bar{\nu})\,d\bar{\nu}\int\epsilon_A(\bar{\nu})\,d\bar{\nu}} \tag{5}$$

where $F_D(\nu)$ is the fluorescence spectrum of the donor and $\epsilon_A(\nu)$ is the extinction coefficient of the acceptor. The overlap integrals were calculated for EET to both first and second singlet states of biacetyl, $S_1$ ($^1A_u$) and $S_2$ ($^1B_g$) respectively. The results are summarized in Table 6. It is clear that the contribution from dipole–dipole Förster-type long-range EET is negligible for the bichromophoric molecules examined, and that the singlet–singlet route has contributions from EET processes to both the $S_1$ and $S_2$ states of the α-diketone.

The triplet–triplet energy differences between the donor and acceptor are 101.6 kJ mol$^{-1}$ for the α-diketone $^3A_u$ state and zero for the $^3B_g$ state [18]. Thus we can assume that triplet–triplet intra-EET in our bichromophoric molecules is to the $^3B_g$ state of the α-diketone and this route will be thermally activated.

Table 6
Experimental results for the spectral overlap integral and the critical distance $R_0$

| Molecule | Transition | $R_0$ (Å) | $J_{ex}$(Dexter) (cm × $10^7$) | $J_{d\text{-}d}$(Förster) (cm$^6$ mol$^{-1}$ × $10^{18}$) |
|---|---|---|---|---|
| Biacetyl | $S_0 \rightarrow S_1$ | 4.35 | 6.50 | 0.112 |
| P-4,4 | | 4.36 | 6.55 | 0.113 |
| P-4,4m | | 4.14 | 4.35 | 0.083 |
| P-5,5 | | 3.92 | 2.55 | 0.060 |
| P-5,5m | | 3.74 | 1.48 | 0.045 |
| Biacetyl | $S_0 \rightarrow S_2$ | 9.03 | 427 | 8.91 |

The singlet–singlet intra-EET process observed for the bichromophoric molecules examined does not reflect any special features which can be attributed to methyl substitution in the bichromophore ring. This is demonstrated by correlating the observed quantum efficiency $Q$ to the interchromophore average distance $R$. This is done by first correcting $Q$ for variations in $J_{ex}$ and for differences in the molecular conformation, as reflected by the temperature dependence of $Q$ following the model based on Dexter-type short-range transfer. The corrected EET quantum efficiencies $Q'$ should follow the relation [17]

$$Q' = \exp(-\beta R) \tag{6}$$

where β is related to the van der Waals' radii of the orbitals. The fitting of the measured $Q'$ values for P-4,4, P-5,5, P-4,4m and P-5,5m is shown in Fig. 10, together with data for other aromatic α-diketone bichromophoric molecules. TB interaction, which when taken into account would have resulted in long-range transfer due to superexchange, was not observed for the singlet–singlet EET route.

The picture for the triplet energy transfer route is more involved and clearly shows that methyl substitution in the interchromophore bridge affects the measured phosphorescence lifetime and phosphorescence spectra. The phosphorescence quantum yield $\Phi_P$ is proportional to the triplet formation quantum yield $\Phi_T$, the phosphorescence lifetime and the triplet radiative lifetime $k_P$

$$\Phi_P = \Phi_T k_P \tau_P \tag{7}$$

We can estimate $\Phi_T$ for the α-diketone chromophore from the absorption and fluorescence spectra using the relation

$$\Phi_T = k_{ISC}\tau_F \tag{8}$$

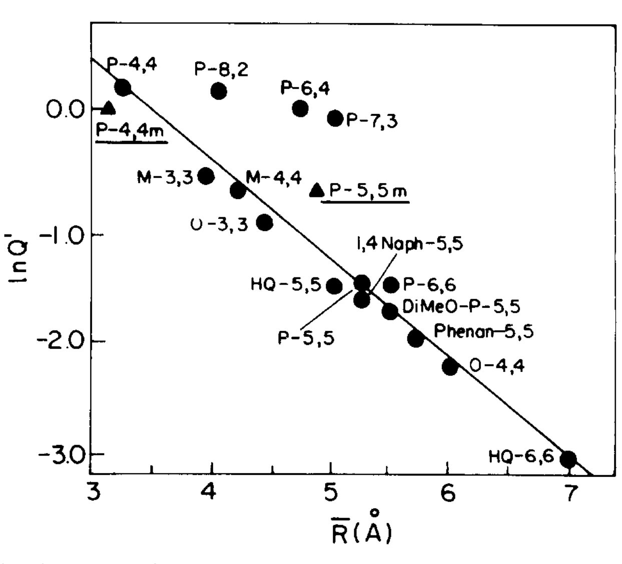

Fig. 10. Plot of ln$Q'$ vs. $R$ for previously studied bichromophoric molecules (●) and presently studied molecules (▲) showing the fit to Eq. (6).

Table 7
Oscillator strength ($f$), fluorescence radiative transition rate $k_F$, fluorescence lifetime $\tau_F$, ISC rate $k_{ISC}$ and quantum yields of triplet formation $\Phi_T$ of the $\alpha$-diketone chromophore calculated by Eq. (8)

| Molecule | $f \times 10^{-4}$ | $k_F$ ($10^5$ s$^{-1}$) | $\tau_F$ (ns) | $k_{ISC}$ ($10^7$ s$^{-1}$) | $\Phi_T$ |
|---|---|---|---|---|---|
| P-4,4 | 6.08 | 2.28 | 16.8 | 5.94 | 0.999 |
| P-4,4m | 6.02 | 2.07 | 14.7 | 6.79 | 0.999 |
| P-5,5 | 5.81 | 2.00 | 15.6 | 6.39 | 0.999 |
| P-5,5m | 5.75 | 1.88 | 12.8 | 7.79 | 0.999 |
| Biacetyl | 6.10 | 2.20 | 14.0 | 7.14 | 0.999 |

while $k_{ISC}$ can be estimated using

$$\frac{1}{\tau_F} = k_{ISC} + k_F + k_{IC} \approx k_{ISC} + k_F \tag{9}$$

The internal conversion rate constant is neglected compared with $k_{ISC}$ in view of the small $S_1$–$T_1$ energy gaps, and $k_F$ is obtained from the absorption data using the oscillator strength relation

$$f = \frac{4m_e c \epsilon_0 n \ln 10}{e^2 N_A} \int \epsilon(\bar{\nu})\, d\bar{\nu} \tag{10}$$

and

$$k_F = \frac{\bar{\nu}^2}{1.5} f \tag{11}$$

where $n$ is the refractive index of the medium, $m_e$ is the mass of an electron, $N_A$ is the Avogadro number and $\nu$ is the frequency of the peak absorption. Table 7 shows the results obtained for the bichromophoric molecules. The $\alpha$-diketone triplet formation yield, which depends on the efficiency of intersystem crossing, is close to unity for all molecules. This is not surprising since all molecules have the same, low, $S_1$–$T_1$ gap of approximately 23 kJ mol$^{-1}$ for similar electronic configurations of the electronic states involved in the process. Eq. (5) predicts a linear relationship between $\Phi_P$ and $\tau_P$. This is exemplified for the bichromophoric molecules in Fig. 11. Since all molecules have the same $\Phi_T$, deviations from linearity can be attributed to differences in $k_P$. It seems that $k_P$ is higher for biacetyl, P-4,4 and P-5,5 than for P-4,4m and P-5,5m. Such an effect of methyl substitution on the oscillator strength for the $S_0 \rightarrow T_1$ transition was observed by McClure [19] for aliphatic ketones. Non-radiative decay of the $\alpha$-diketone triplet state is less efficient for the methyl-substituted molecules. This result may be due to either or both of the following effects. Calculations show that methyl substitution reduces the flexibility of the interchromophore bridge thus reducing the probability of intramolecular non-radiative triplet decay. Richtol and Klappmeier [20] showed, in a series of aliphatic diketones of increasing chain length, that increasing the chain length had no effect on the fluorescence yield, but that the phosphorescence intensity of 2,3-octanedione was reduced by two orders of magnitude compared with biacetyl. Alternatively, the effect on the non-radiative decay of methyl-substituted diketones may be ascribed to the intervention of a new deactivation pathway, namely intramolecular photochemical reaction of the methylated compounds [21]. (Inefficient photochemical reaction of P-5,5m, but not P-4,4m, has been observed on irradiation at λ > 400 nm [22].)

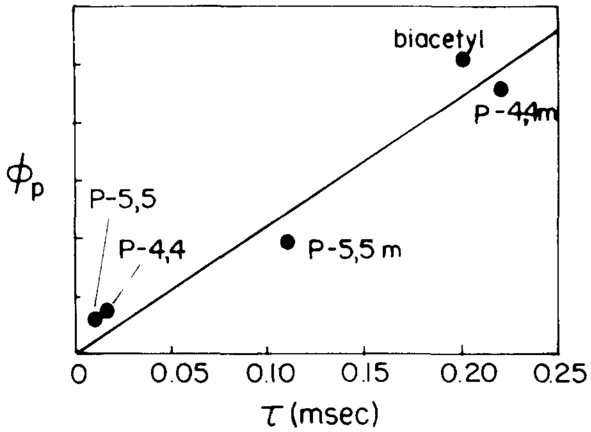

Fig. 11. Relative phosphorescence quantum yield vs. measured phosphorescence lifetime together with linear regression fit ($R = 0.95$).

We now turn to intra-EET and, in particular, to the triplet transfer route, where our results indicate that methyl substitution $\beta$ to the acceptor carbonyls in the bichromophoric bridge has an effect on the apparent transfer efficiency. For the singlet–singlet EET route, no such effect was observed. The quantum yield for donor triplet formation ($\Phi_T(D)$) can be estimated from the relation

$$\Phi_T(D) = \frac{k_{ISC}{}^{D}}{\sum k + k_{ET}{}^{SS}} \tag{12}$$

where $k_{ISC}{}^{D}$ is the intersystem crossing rate constant of the donor and sum$k$ denotes the sum of the rate constants of all radiative and non-radiative decay processes of the donor, excluding the singlet–singlet intra-EET rate constant $k_{ET}{}^{SS}$. Using Eq. (12) and the results for the singlet–singlet intra-EET quantum yields, we find that $\Phi_T(D)$ is 0.07 for P-5,5 and 0.007 for all other bichromophoric molecules. Since triplet yield formation for the acceptor is $\Phi_T(A) \approx 1$ for all bichromophoric molecules, this implies that the observed high $\xi^{T\text{-}T}$ values for P-4,4 and P-5,5 are due to a significant contribution from singlet donor to triplet acceptor EET, in addition to some contribution from triplet–triplet intra-EET. No enhancement of the phosphorescence of the acceptor chromophore as a result of intra-EET was observed for P-4,4m and P-5,5m, in agreement with the observed short phosphorescence lifetimes for these molecules compared with P-4,4 and P-5,5 and the lack of temperature dependence of the phosphorescence yield of the acceptor chromophore on donor excitation. However, it is difficult to relate this observation to hindered TB interaction in P-4,4 and P-5,5 alone, because the effect can also be rationalized in terms of more efficient triplet non-radiative decay of P-4,4m and P-5,5m, or a contribution from a photochemical reaction; in other words, this could be the rate-determining step rather than intra-EET.

## 5. Conclusions

We have presented results on the intra-EET in bichromophoric molecules in which the interchromophore bridge contains methyl substituents $\beta$ to the $\alpha$-dicarbonyl acceptor chromophore. The results show that singlet–singlet intra-EET is independent of substitution and can be explained by a model assuming Dexter-type short-range exchange interaction. For singlet–triplet and triplet–triplet transfer, there are indications that the phosphorescence yield of the acceptor is larger for the non-substituted bichromophoric molecules. This can be explained by TB interaction promoting EET via a long-range superexchange mechanism, by variations in the non-radiative decay of the triplet state of the acceptor or by chemical reaction.

## Acknowledgments

This work was supported in part by the Fund for Promotion of Research at the Technion. We thank Professor R. Gleiter, University of Heidelberg, for the samples of P-4,4m and P-5,5m.

## References

[1] N.J. Turro, *Modern Molecular Photochemistry*, Benjamin, London, 1978.

[2] (a) N. Mataga and T. Kubota, *Molecular Interactions and Electronic Spectra*, Dekker, New York, 1970. (b) J. Klafter and A. Blumen, *J. Chem. Phys., 84* (1986) 1397. (c) M.A. Ali and S.A. Ahmed, *J. Chem. Phys., 90* (1989) 1397.

[3] L.I. Schiff, *Quantum Mechanics*, McGraw-Hill, New York, 1949.

[4] Th. Förster, *Discuss. Faraday Soc., 27* (1959) 7.

[5] S. Speiser, *J. Photochem., 22* (1983) 195.

[6] G.D. Scholes, A.H.A. Clayton and K.P. Ghiggino, *J. Chem. Phys., 97* (1992) 7405.

[7] J.W. Verhoeven, *Pure Appl. Chem., 62* (1990) 1585.

[8] (a) H. Oevering, J.W. Verhoeven, M.N. Paddon-Row, N.S. Husch and E. Cotsaris, *Chem. Phys. Lett., 143* (1988) 488. (b) H. Oevering, J.W. Verhoeven, M.N. Paddon-Row, N.S. Hush and E. Cotsaris, *Chem. Phys. Lett., 150* (1988) 179. (c) J. Kroon, A.M. Oliver, J.W. Verhoeven and M.N. Paddon-Row, *J. Am. Chem. Soc., 112* (1990) 4868.

[9] (a) G.L. Closs, P. Piotrowiak, J.M. MacInnis and G.R. Fleming, *J. Am. Chem. Soc., 110* (1988) 2652. (b) G.L. Closs, D.M. Johnson, J.R. Miller and P. Piotrowiak, *J. Am. Chem. Soc., 111* (1989) 3751.

[10] H. Oevering, J.W. Verhoeven, M.N. Paddon-Row, N.S. Husch, M. Heppener, A.M. Oliver and E. Cotsaris, *J. Am. Chem. Soc., 109* (1987) 3285, and references cited therein.

[11] G.D. Scholes, K.P. Ghiggino, A.M. Oliver and M.N. Paddon-Row, *J. Phys. Chem., 97* (1993) 11 871.

[12] S.T. Levy, M.B. Rubin and S. Speiser, *J. Am. Chem. Soc., 114* (1992) 10 747.

[13] S.T. Levy, M.B. Rubin and S. Speiser, *J. Photochem. Photobiol. A: Chem., 66* (1992) 159.

[14] S.T. Levy, Intramolecular electronic energy transfer in bichromophoric molecules, *M.Sc. Thesis*, Technion, 1991.

[15] S.T. Levy and S. Speiser, *J. Chem. Phys., 96* (1992) 3585.

[16] D.L. Dexter, *J. Chem. Phys., 21* (1953) 836.

[17] (a) S. Hassoon, H. Lustig, M.B. Rubin and S. Speiser, *J. Phys. Chem., 88* (1984) 6367. (b) S. Hassoon, Photophysics and photochemistry of cyclic $\alpha$-diketones, *D.Sc. Thesis*, Technion, 1984.

[18] (a) J.B. Birks, *Photophysics of Aromatic Molecules*, Wiley, New York, 1970. (b) J.B. Birks, *Organic Molecular Photophysics*, Vol. 1, Wiley, New York, 1973, p. 327. (c) J.B. Birks, *Organic Molecular Photophysics*, Vol. 2, Wiley, New York, 1975.

[19] D.S. McClure, *J. Chem. Phys., 17* (1949) 905.

[20] H.H. Richtol and F.H. Klappmeier, *J. Chem. Phys., 44* (1966) 1519.

[21] (a) W.W. Urry and D.J. Trecker, *J. Am. Chem. Soc., 84* (1962) 118. (b) W.W. Urry, D.J. Trecker and D.A. Winey, *Tetrahedron Lett.*, (1962) 609.

[22] R. Kramer, unpublished results, 1990.